Supporting information

Co-doped modified $LiLuF_4$:Eu microcrystalline scintillation with flexible film for high resolution X-ray imaging

Xixi Huang[a], Jinhai Yang[a], Hao Lu[b,c], Xieming Xu[b,d], Shuaihua Wang[b,d,] and Shaofan Wu[b,d]*

a. College of Chemistry, Fuzhou University, Fuzhou, 350108, PR China.

b. Key Laboratory of Optoelectronic Materials Chemistry and Physics, Fujian Institute of Research on the Structure of Matter, Chinese Academy of Sciences, Fuzhou, 350002, China

c. University of the Chinese Academy of Sciences, Beijing 100049, China

d. Fujian Science & Technology Innovation Laboratory for Optoelectronic Information of China, Fuzhou, Fujian 350108, China

Table S1. Comparison of the detection limit of reported scintillators

Scintillators	The detection limit [nGy s^{-1}]	References
$LiYbF_4$:Tb NCs	360	[1]
$[TPPen]_2Mn_{0.9}Zn_{0.1}Br_4$	204.1	[2]
$[FEtQ]_2MnBr_4$	258	[3]
K_2CuBr_3	132.82	[4]
$Cs_2AgBiCl_6$	241	[5]
$LiLuF_4$:Eu,Gd	140.72	This work

References: [1] CrystEngComm, 2022, 24, 2551–2557. [2] Adv. Optical Mater. 2023, 2300330. [3] Adv. Funct. Mater. 2021, 31, 2102848. [4] ACS Appl. Electron. Mater. 2020, 2, 2242−2249. [5] ACS Appl. Electron. Mater. 2022, 4, 4530−4539.

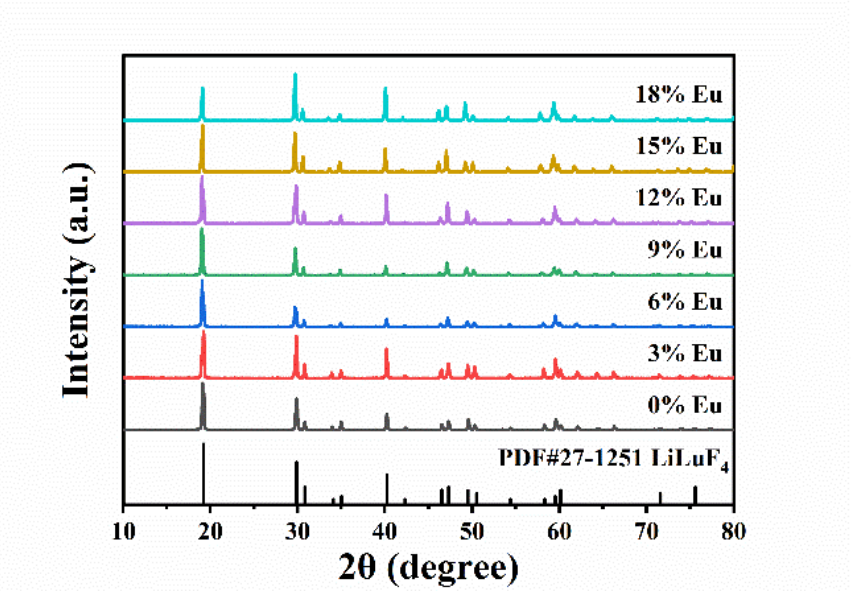

Fig. S1 XRD patterns of $LiLuF_4$:x%Eu MCs with different Eu^{3+} contents.

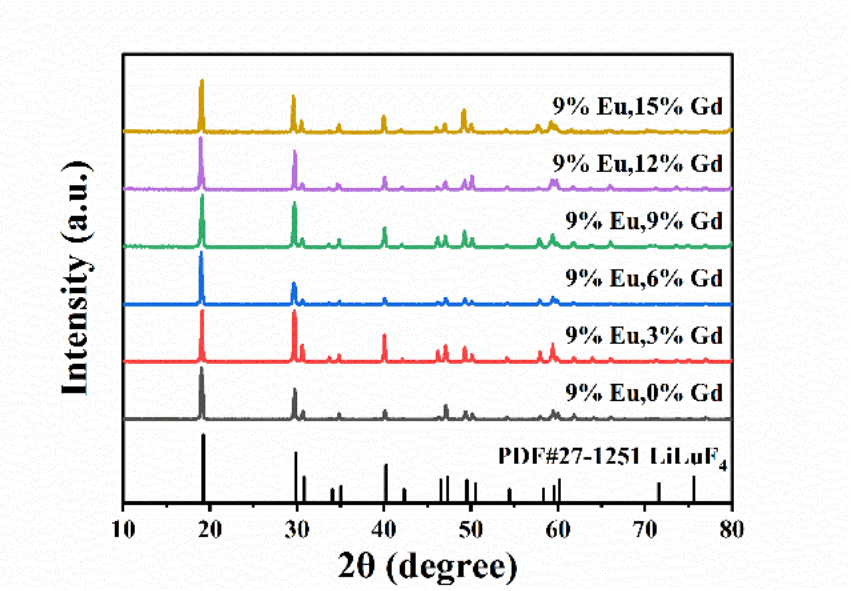

Fig. S2 XRD patterns of $LiLuF_4$:9%Eu,x%Gd MCs with different Gd^{3+} contents.

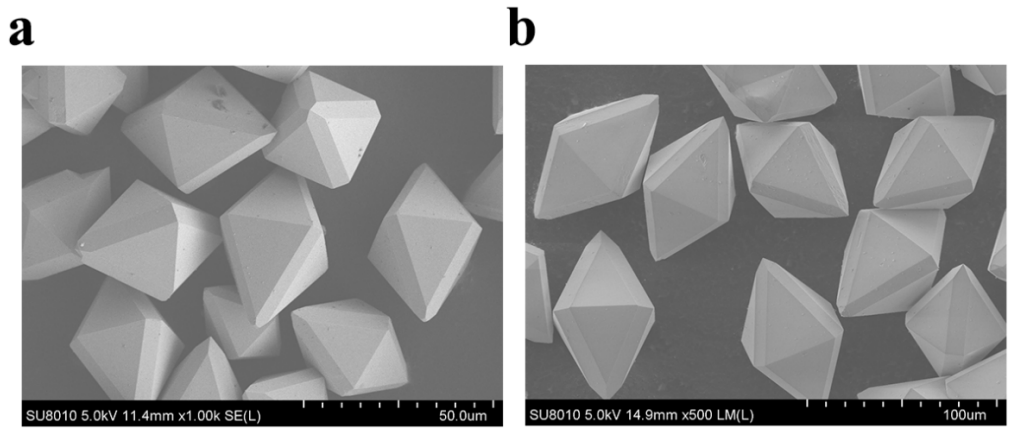

Fig. S3 Partial SEM image of $LiLuF_4$:9%Eu MCs (a) and $LiLuF_4$:9%Eu,12%Gd MCs (b).

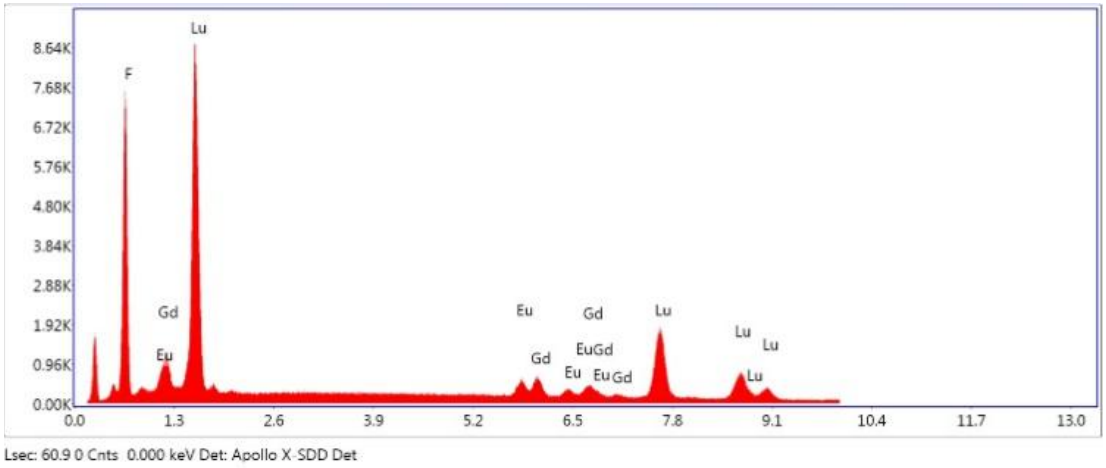

Fig. S4 The EDS of the $LiLuF_4$:9%Eu,12%Gd MCs.

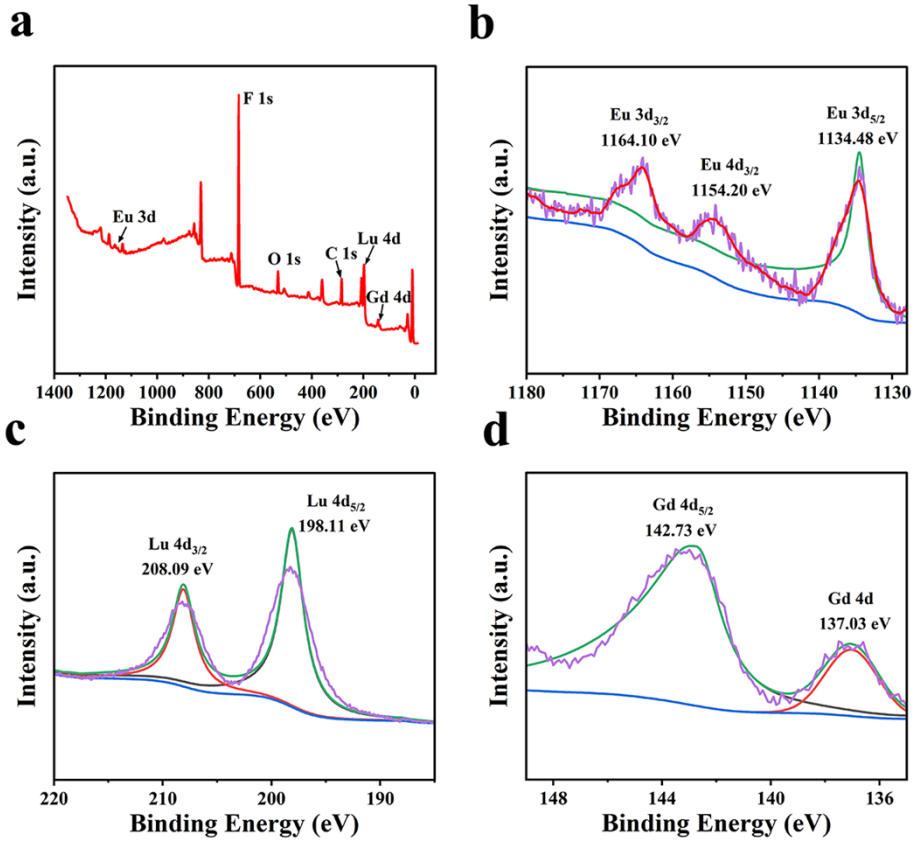

Fig. S5 Full XPS spectra of (a) $LiLuF_4$:9%Eu,12%Gd MCs and high-resolution XPS spectra of (b) Eu 3d, (c) Lu 4d, (d) Gd 4d.

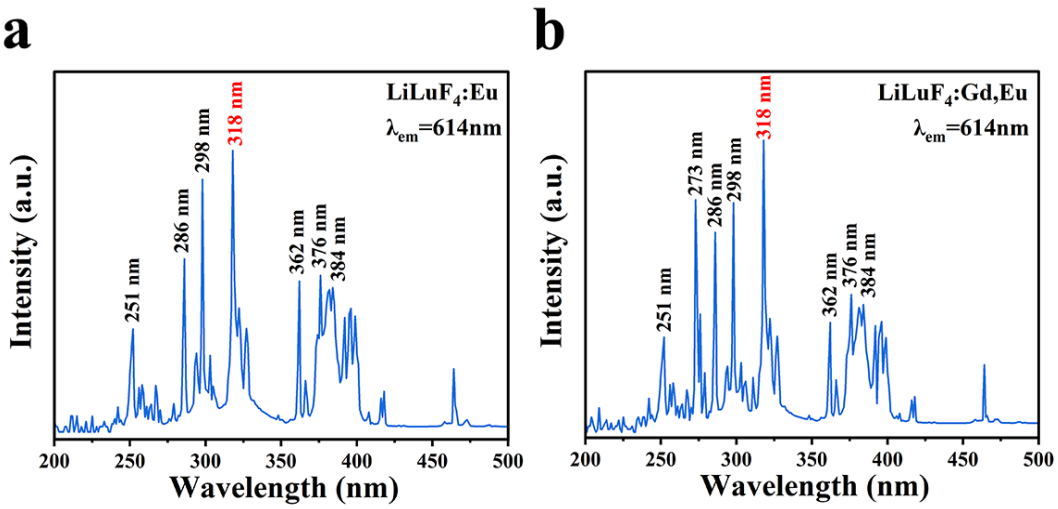

Fig. S6 The excitation spectrum of $LiLuF_4$:9%Eu and $LiLuF_4$:9%Eu,12%Gd MCs.

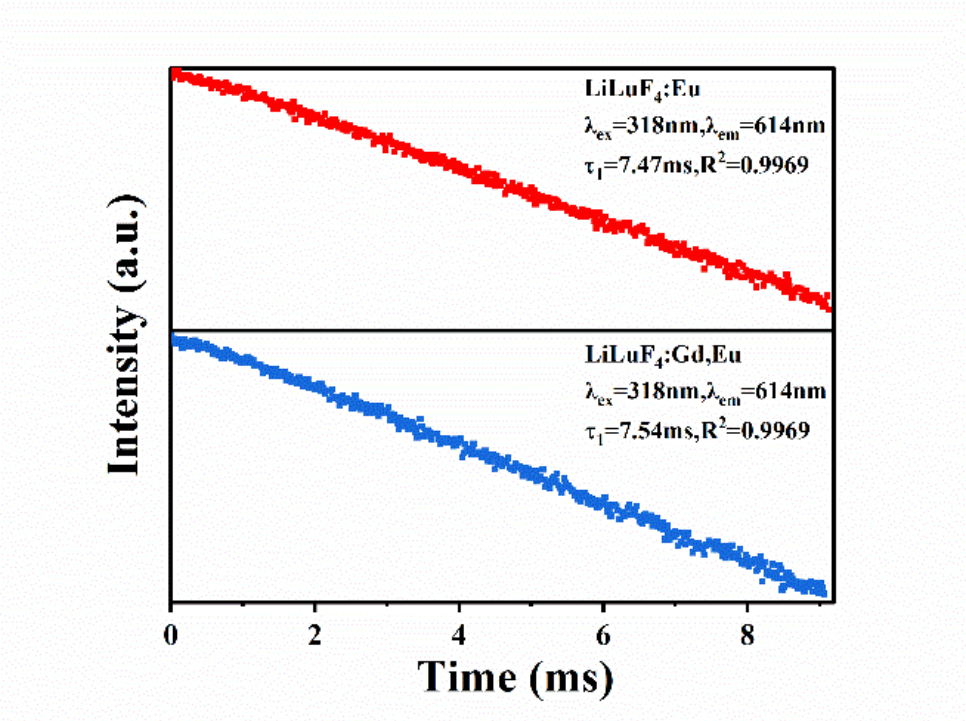

Fig. S7 Photoluminescence decay spectra of $LiLuF_4$:9%Eu (top) and $LiLuF_4$:9%Eu,12%Gd (bottom).

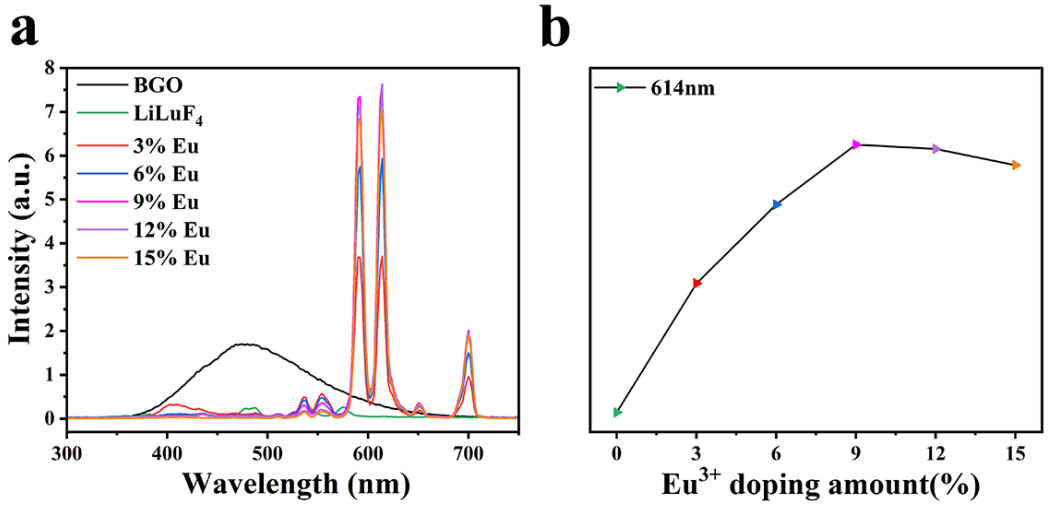

Fig. S8 X-ray luminescence spectra of $LiLuF_4$:x%Eu and BGO at X-ray dose rate 42.29 mGy/s.

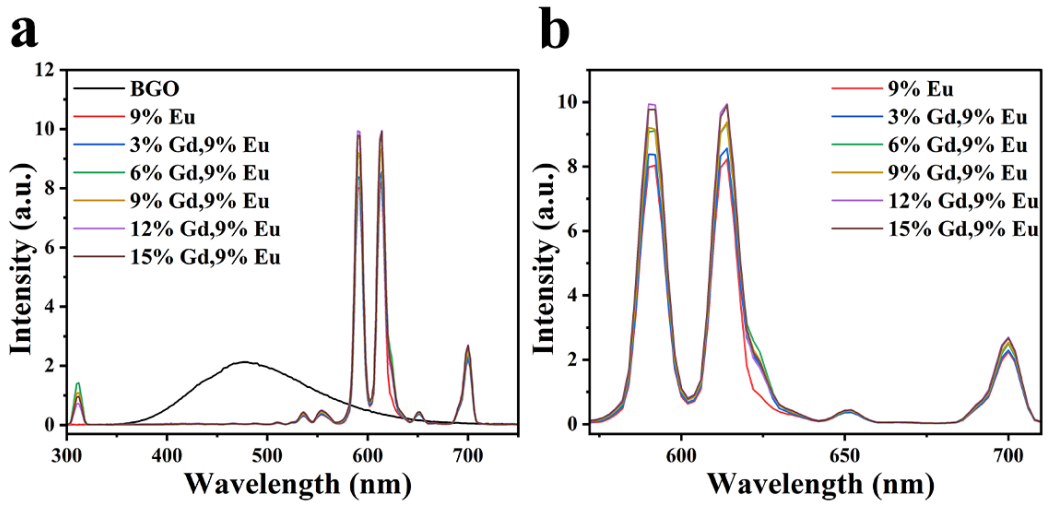

Fig. S9 X-ray luminescence spectra of $LiLuF_4$:x%Gd,9%Eu and BGO at X-ray dose rate 42.29 mGy/s.

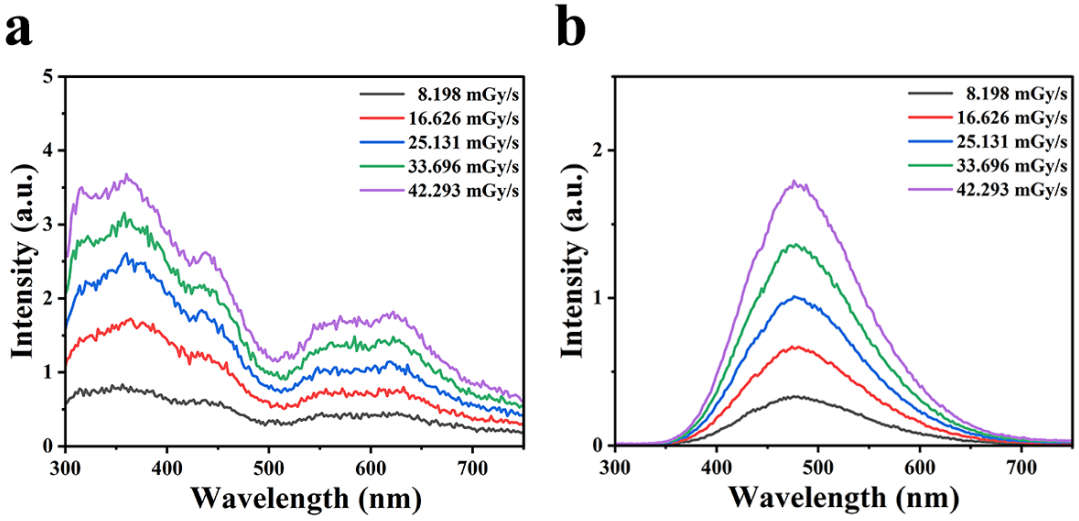

Fig. S10 The radioluminescence spectra of BaF_2 (a) and BGO (b) at a voltage of 50kV and a dose rate of 8.198mGy/s～42.293 mGy/s.

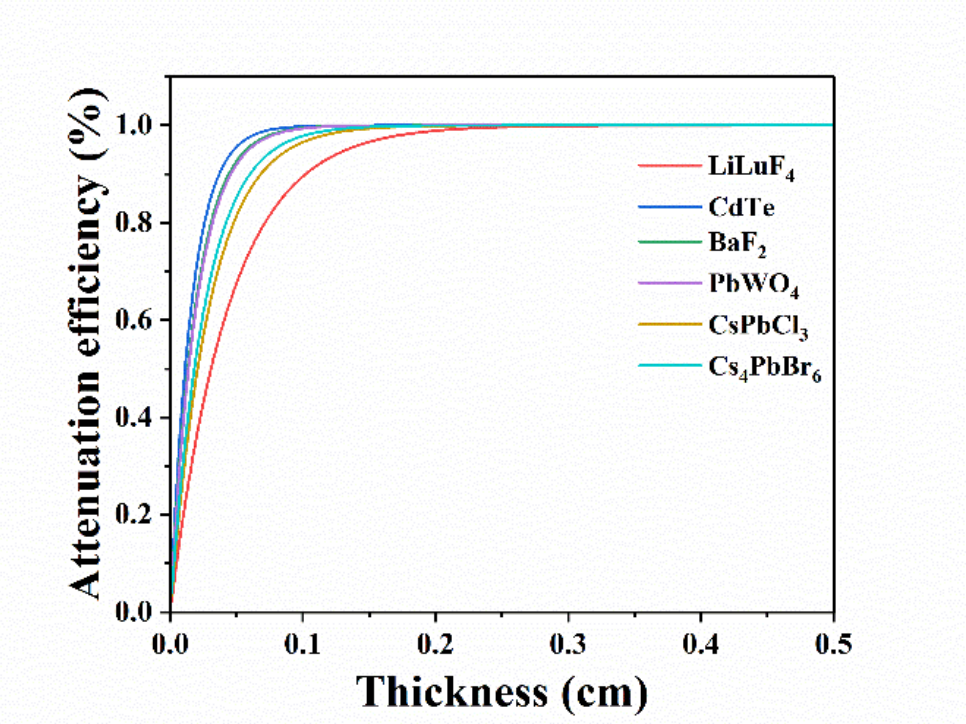

Fig. S11 Attenuation efficiencies as a function of the material thickness of $LiLuF_4$ and several scintillators to 50 keV X-ray photons.

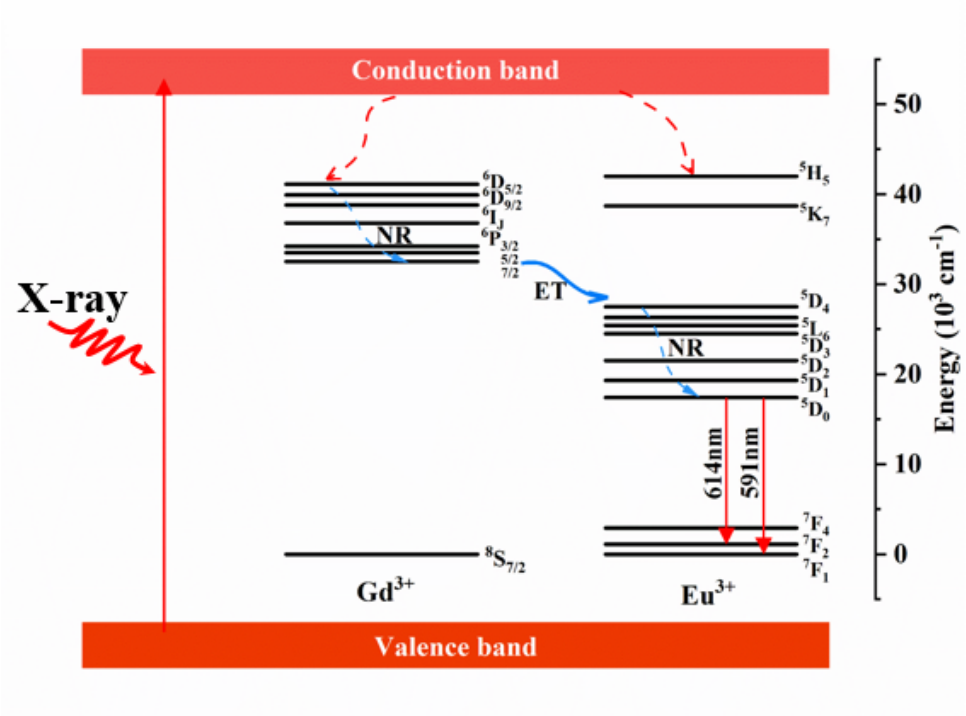

Fig. S12 The energy level transition process of Eu^{3+} and Gd^{3+}.

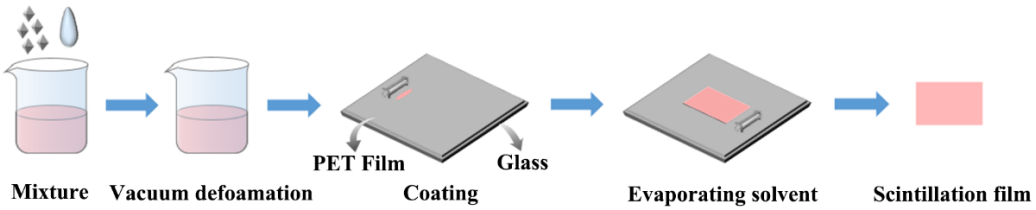

Fig. S13 Schematic diagram of preparation process of $LiLuF_4$:9%Eu,12%Gd MCs-EP composite scintillating film.

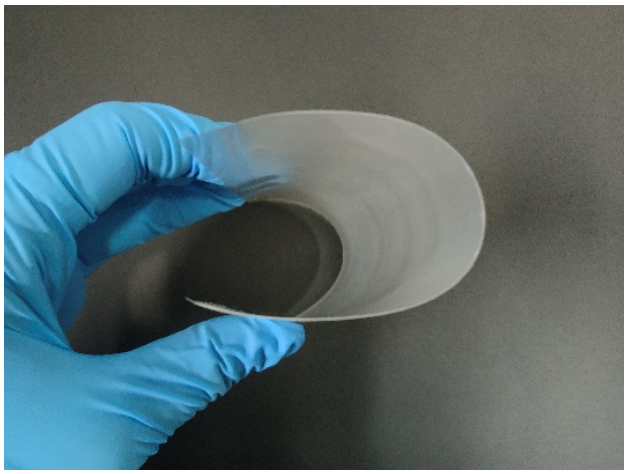

Fig. S14 The physical image of 50wt% $LiLuF_4$:9%Eu,12%Gd scintillation film.

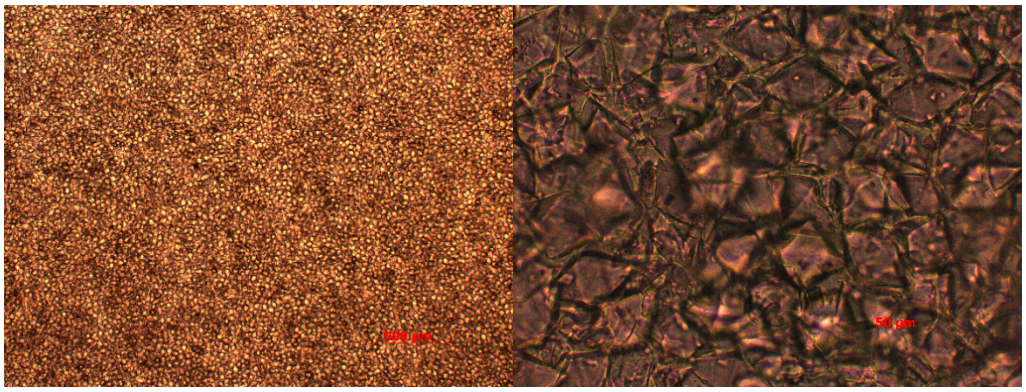

Fig. S15 The grain distribution of $LiLuF_4$:9%Eu,12%Gd film observed under a microscope.

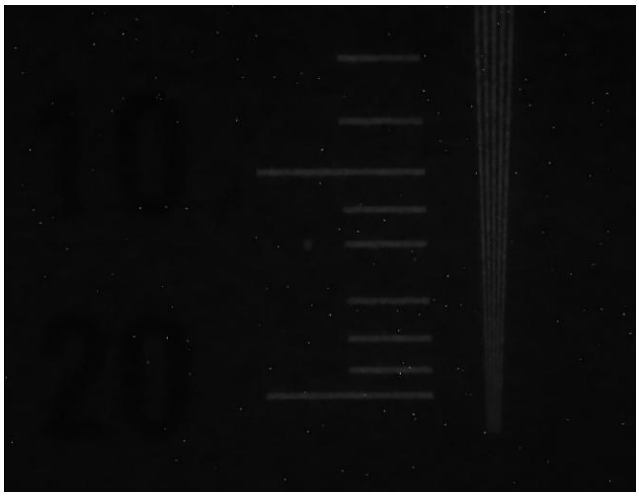

Fig. S16 The grayscale image at 10-20 LP/mm of $LiLuF_4$:9%Eu,12%Gd scintillation film.

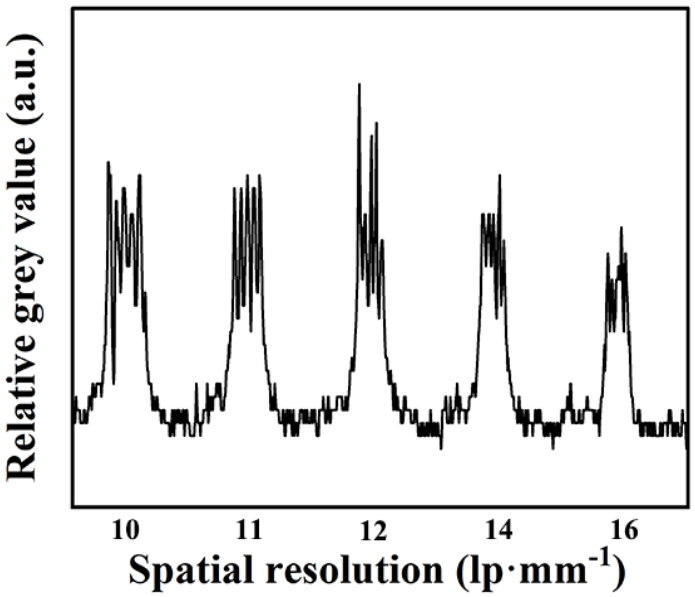

Fig. S17 The stripe brightness extraction map of $LiLuF_4$:9%Eu,12%Gd film at 10-16 LP/mm.

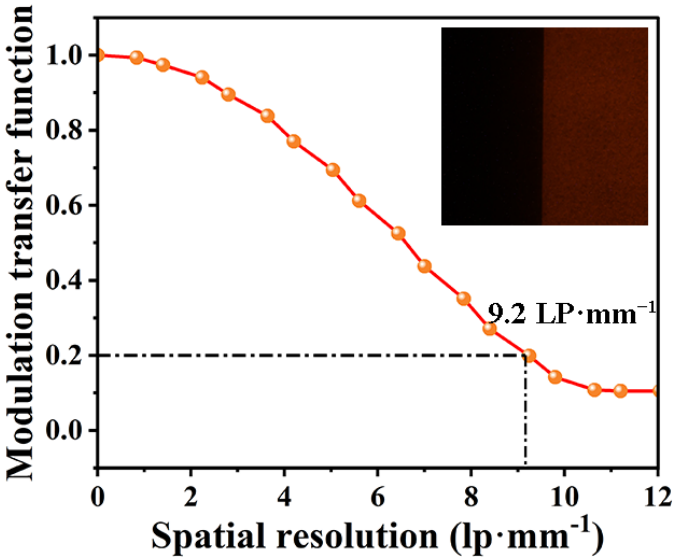

Fig. S18 Modulation transfer functions (MTF) of the X-ray edge image obtained by $LiLuF_4$:9%Eu film.